Supplemental Information (*SI*) for

Silencing of Retrotransposon-derived Imprinted Gene *RTL1* is the Main Cause for Post-implantational Failures in Mammalian Cloning

This PDF file includes:

Figs. S1 to S16

Table S1

www.pnas.org/cgi/doi/10.1073/pnas.1814514115

Figure S1

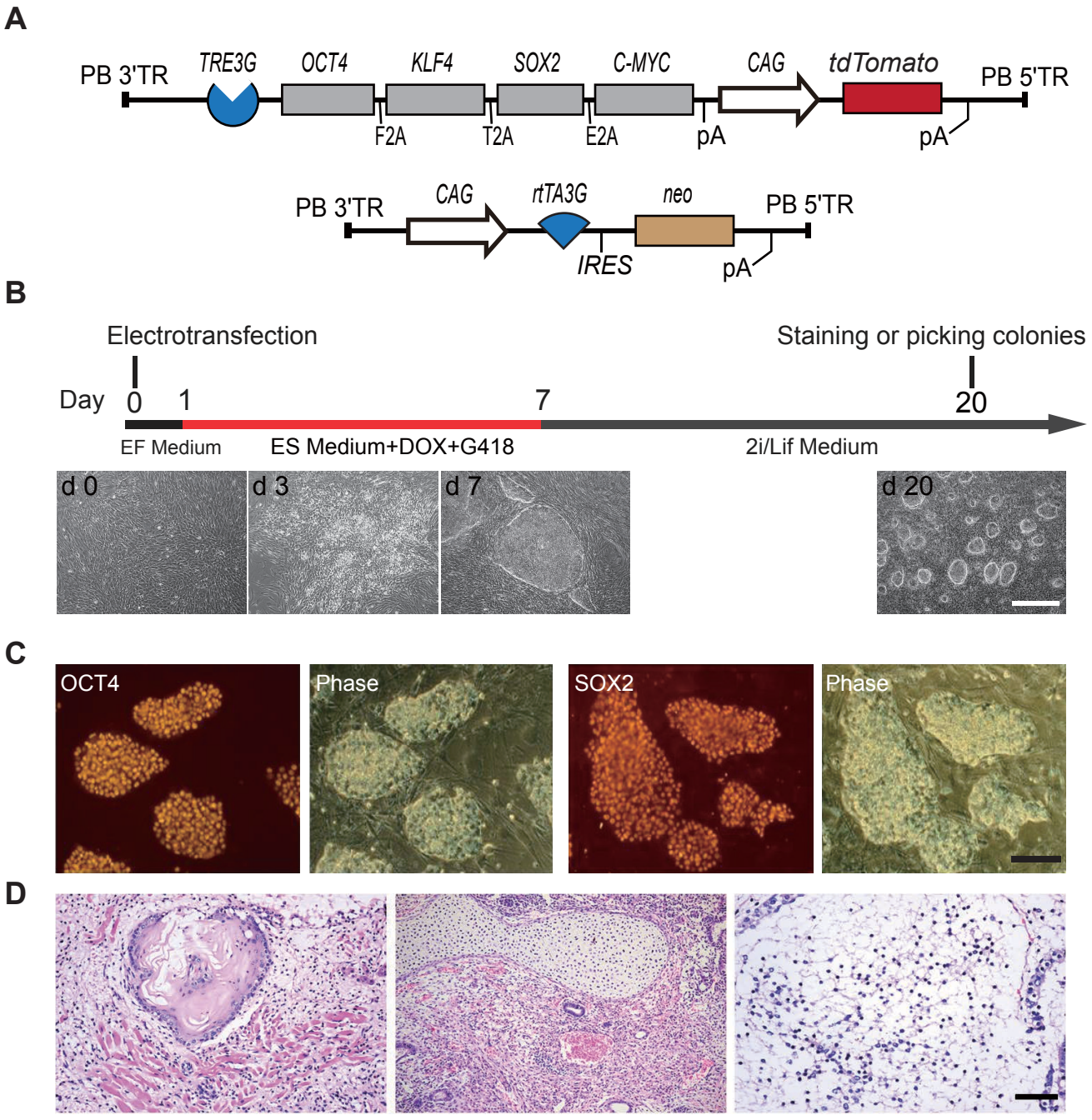
A
PB 3'TR
TRE3G
OCT4
KLF4
SOX2
C-MYC
CAG
tdTomato
PB 5'TR
F2A
T2A
E2A
pA
pA
PB 3'TR
CAG
rtTA3G
neo
PB 5'TR
IRES
pA
B
Electrotransfection
Staining or picking colonies
Day 0 1 7 20
EF Medium
ES Medium+DOX+G418
2i/Lif Medium
d 0
d 3
d 7
d 20
C
OCT4
Phase
SOX2
Phase
D

Fig. S1. Derivation of pig iPSCs using the DOX-inducible system.

(A) Schematic representation of the DOX-inducible system for iPSC induction. The top is a *piggyBac* vector containing *OCT4-KLF4-SOX2-C-MYC* (*OSKM*) under control of the TRE3G promoter. The bottom is a *piggyBac* vector containing the reverse transactivator rtTA3G.

(B) Timeline of reprogramming with the DOX-inducible system. Representative primary clones formed at day 7 after transfection. Pig iPSCs in 2i/LIF+DOX medium showed mouse ES-like tight three-dimensional clones at day 20. EF medium, serum-based embryonic fibroblast medium; ES medium, serum/LIF based ESC medium; 2i/LIF, serum-free ESC medium supplemented with PD0325901, CHIR90021, and LIF. Scale bar, 500 μm.

(C) Immunofluorescence staining of pluripotency markers, OCT4 and SOX2, in iPSCs cultured on irradiated mouse fibroblasts. Scale bar, 100 μm.

(D) Hematoxylin and eosin staining of paraffin sections of teratomas generated from porcine iPS cells. Scale bar, 500 μm.

Figure S2

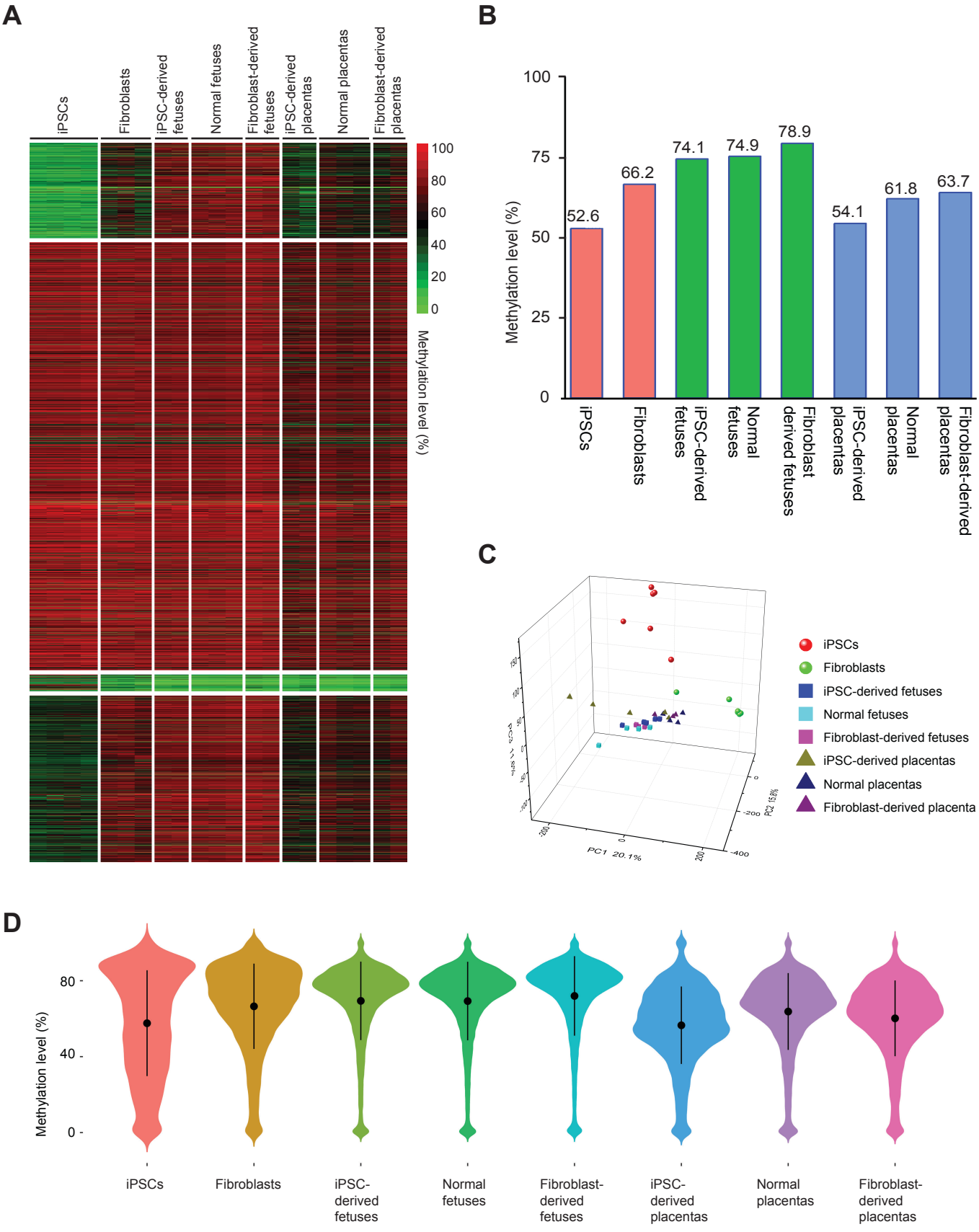
A
iPSCs
Fibroblasts
iPSC-derived fetuses
Normal fetuses
Fibroblast-derived fetuses
iPSC-derived placentas
Normal placentas
Fibroblast-derived placentas
100
80
60
40
20
0
Methylation level (%)
B
Methylation level (%)
100
75
50
25
0
52.6
66.2
74.1
74.9
78.9
54.1
61.8
63.7
iPSCs
Fibroblasts
iPSC-derived fetuses
Normal fetuses
Fibroblast derived fetuses
iPSC-derived placentas
Normal placentas
Fibroblast-derived placentas
C
PC1 20.1%
PC2 15.8%
iPSCs
Fibroblasts
iPSC-derived fetuses
Normal fetuses
Fibroblast-derived fetuses
iPSC-derived placentas
Normal placentas
Fibroblast-derived placenta
D
Methylation level (%)
80
40
0
iPSCs
Fibroblasts
iPSC-derived fetuses
Normal fetuses
Fibroblast-derived fetuses
iPSC-derived placentas
Normal placentas
Fibroblast-derived placentas

Fig. S2. Patterns of the DNA methylome in pig nuclear transfer conceptuses.

(A) Clustered heat map showing the methylation pattern of all WGBS samples. Each line indicates the gene body methylation level for all pig Ensembl genes.

(B) Bar plots of methylation level for different pig tissues. Each bar represents the average methylation level of all the CpG sites.

(C) Principal component analysis (PCA) based on the gene expression of all samples. PCA 3D scatter plots were generated based on the gene expression (FPKM) of all genes in all lncRNA-seq porcine samples (including 6 iPSCs, 7 fibroblasts, 5 iPSC-derived fetuses, 3 fibroblast-derived fetuses, 4 normal fetuses, 5 iPSC-derived placentas, 3 fibroblast-derived placentas, 4 normal placentas). 47.5% of the total variance was explained by the first three PCs (PC1, 20.1%; PC2, 15.8%; PC3, 11.6%).

(D) Violin plots for methylation level of all Ensembl genes in different pig tissues. The plots show the distribution for gene body methylation level of all genes in pig tissues. The methylation distribution difference is dramatically evened out after NT. The X-axis represents the probability density of the data at each methylation level. The mean and SD are indicated by the white dots and error bars.

Figure S3

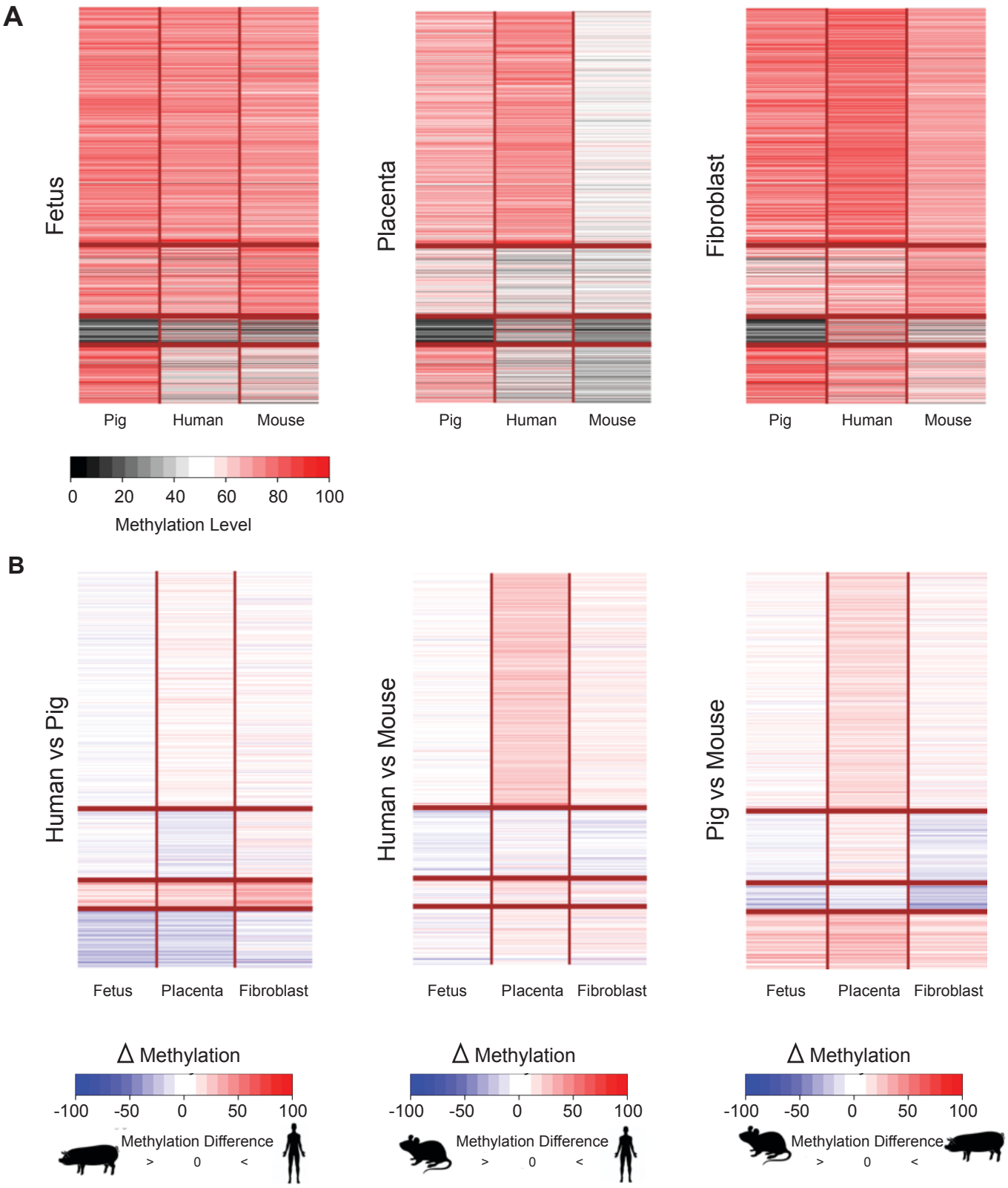
A
Fetus
Placenta
Fibroblast
Pig
Human
Mouse
0
20
40
60
80
100
Methylation Level
B
Human vs Pig
Human vs Mouse
Pig vs Mouse
Fetus
Placenta
Fibroblast
Δ Methylation
-100
-50
0
50
100
Methylation Difference
>
0
<

Fig. S3. Global methylation patterns of pig genome are similar to human.

(A) Heat map for the methylation level of gene body clustered by tissue type in the pig with equivalent methylation values for orthologous sequences in mouse and human. The color keys from black to red indicate low to high methylation level.

(B) The Δ methylation heat map displays the difference in methylation from the cross-species comparison (Δ methylation = right species – left species). The color keys from blue to red indicate hypomethylation to hypermethylation difference between two species.

Figure S4

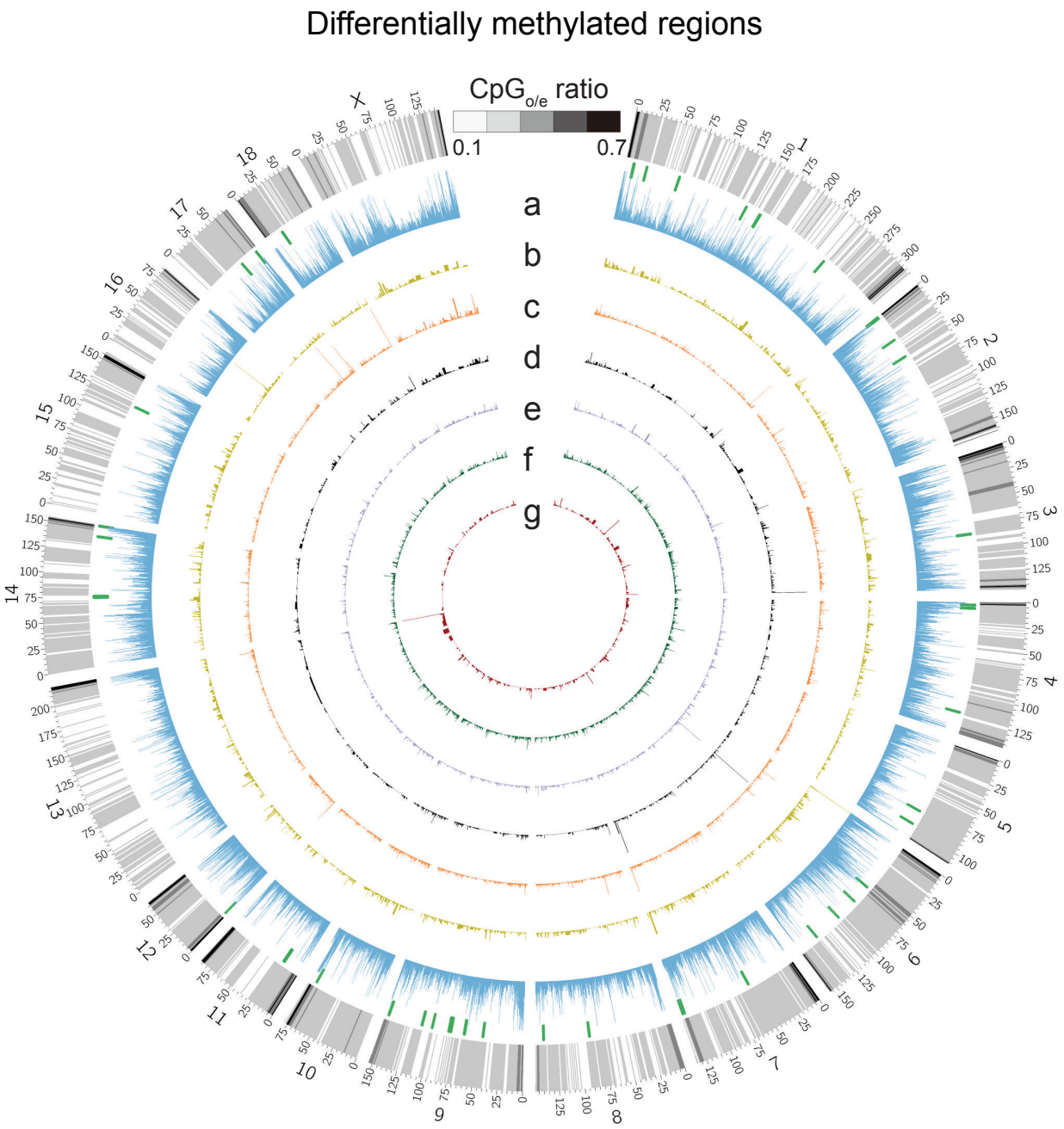

a. Fibroblasts vs. iPSCs

b. iPSC-derived fetuses vs. Normal fetuses

c. iPSC-derived fetuses vs. Fibroblast-derived fetuses

d. Fibroblast-derived fetuses vs. Normal fetuses

e. iPSC-derived placentas vs. Normal placentas

f. iPSC-derived placentas vs. Fibroblast-derived placentas

g. Fibroblast-derived placentas vs. Normal placentas

Fig. S4. An overall view of genome-wide distribution of pairwise DMRs.

The outermost circle displays pig chromosomes and the CpGo/e ratio at 1 Mb bins. The second circle displays the 62 known and candidate imprinted loci (green). The third to ninth circles represent 9 categories of DMRs (a: Fibroblast vs. iPSC DMR, b: iPSC-derived fetus vs. Normal fetus, c: iPSC-derived fetus vs. Fibroblast-derived fetus, d: Fibroblast-derived fetus vs. Normal fetus, e: iPSC-derived placenta vs. Normal placenta, f: iPSC-derived placenta vs. Fibroblast-derived placenta, g: Fibroblast-derived placenta vs. Normal Placenta).

Figure S5

All candidate imprinted DMRs and imprinted genes identified in this study

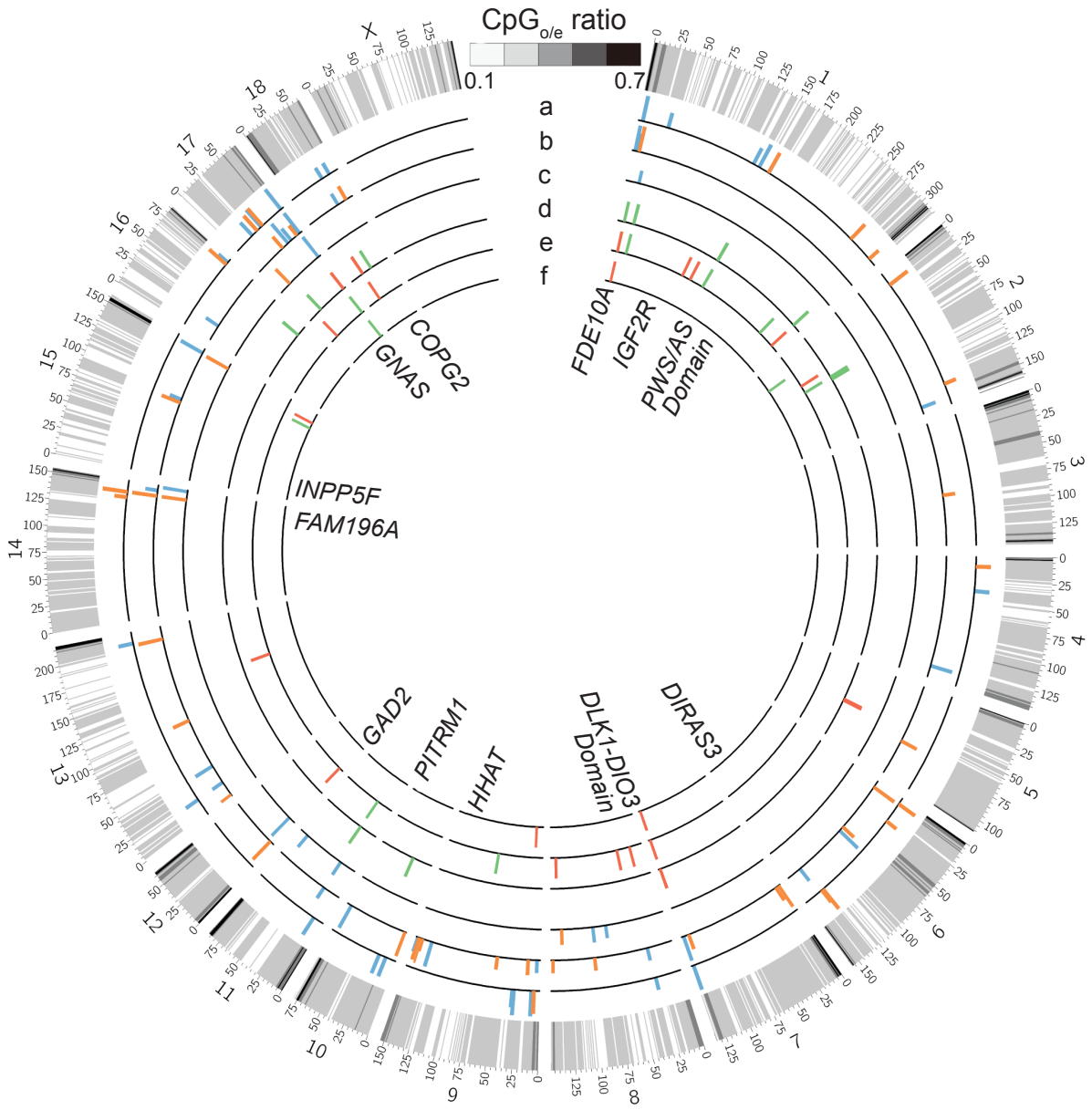

a. Fetus imprinted DMRs

b. Placenta imprinted DMRs

c. Fibroblast imprinted DMRs

d. Fetus imprinted genes

e. Placenta imprinted genes

f. Fibroblast imprinted genes

Fig. S5. Circular representation of the genome-wide distribution of all candidate imprinted DMRs and imprinted genes identified in this study.

The outermost circle displays pig chromosomes and the CpG observed/expected ratio (CpGo/e) in 1 Mb bins. The second to fourth circles represent 3 categories of imprinted DMRs (a: Fetus imprinted DMRs, b: Placenta imprinted DMRs, c: Fibroblast imprinted DMRs). The height of the histogram bins indicates the number of CpGs in the imprinted DMRs. Blue bars: DMRs with paternal methylation; Orange bars: maternal methylation. The fifth to seventh circles represent 3 categories of imprinted genes (d: Imprinted genes in Fetus, e: Imprinted genes in placenta, f: Imprinted genes in Fibroblast). Green ticks: imprinted genes with paternal expression; Red ticks: maternal expression. Imprinted genes are generally in cluster distribution and some examples of imprinted cluster are shown.

Figure S6

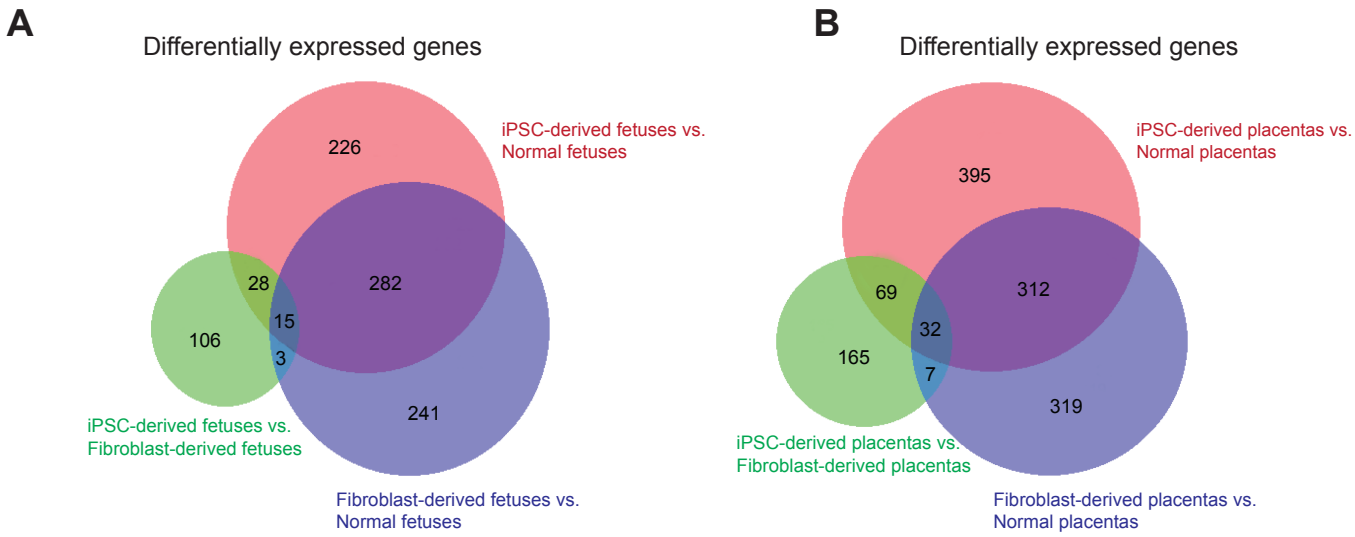
A
Differentially expressed genes
226
iPSC-derived fetuses vs.
Normal fetuses
28
282
15
106
3
241
iPSC-derived fetuses vs.
Fibroblast-derived fetuses
Fibroblast-derived fetuses vs.
Normal fetuses
B
Differentially expressed genes
395
iPSC-derived placentas vs.
Normal placentas
69
312
32
165
7
319
iPSC-derived placentas vs.
Fibroblast-derived placentas
Fibroblast-derived placentas vs.
Normal placentas

Fig. S6. Differentially expressed genes in fetuses and placentas.

(A) Venn diagram showing the overlap of DEGs (including coding genes and lncRNAs) detected by pairwise comparison among iPSC-derived fetus, fibroblast-derived fetus, and normal fetus.

(B) Venn diagram showing the overlap of DEGs (including coding genes and lncRNAs) detected by pairwise comparison among iPSC-derived placenta, fibroblast-derived placenta, and normal placenta.

Figure S7

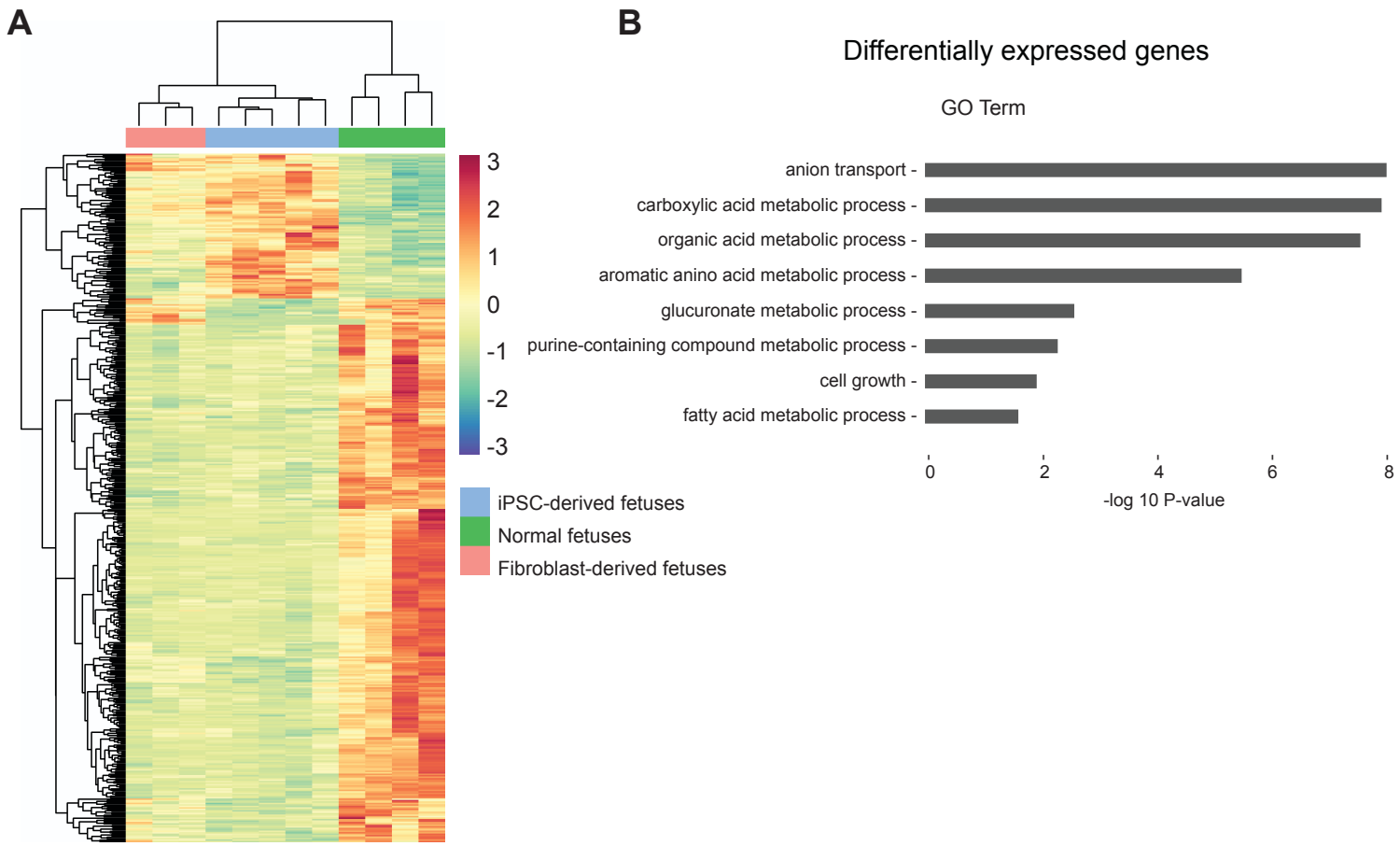
A
3
2
1
0
-1
-2
-3
iPSC-derived fetuses
Normal fetuses
Fibroblast-derived fetuses
B
Differentially expressed genes
GO Term
anion transport -
carboxylic acid metabolic process -
organic acid metabolic process -
aromatic anino acid metabolic process -
glucuronate metabolic process -
purine-containing compound metabolic process -
cell growth -
fatty acid metabolic process -
0
2
4
6
8
-log 10 P-value

Fig. S7. Analysis of (DEGs) between iPSC-derived fetuses and normal fetuses .

(A) Heat map represents the expression profiles of DEGs between iPSC-derived fetus and normal fetus (DESeq2 adjusted P value, 0.001). Genes were subjected to hierarchical clustering.

(B) Gene ontology analysis of the DEGs between iPSC-derived fetus and normal fetus. The x-axis represents the negative log of the P values (classic Fisher's test) of the enrichment of the corresponding gene ontology terms.

Figure S8

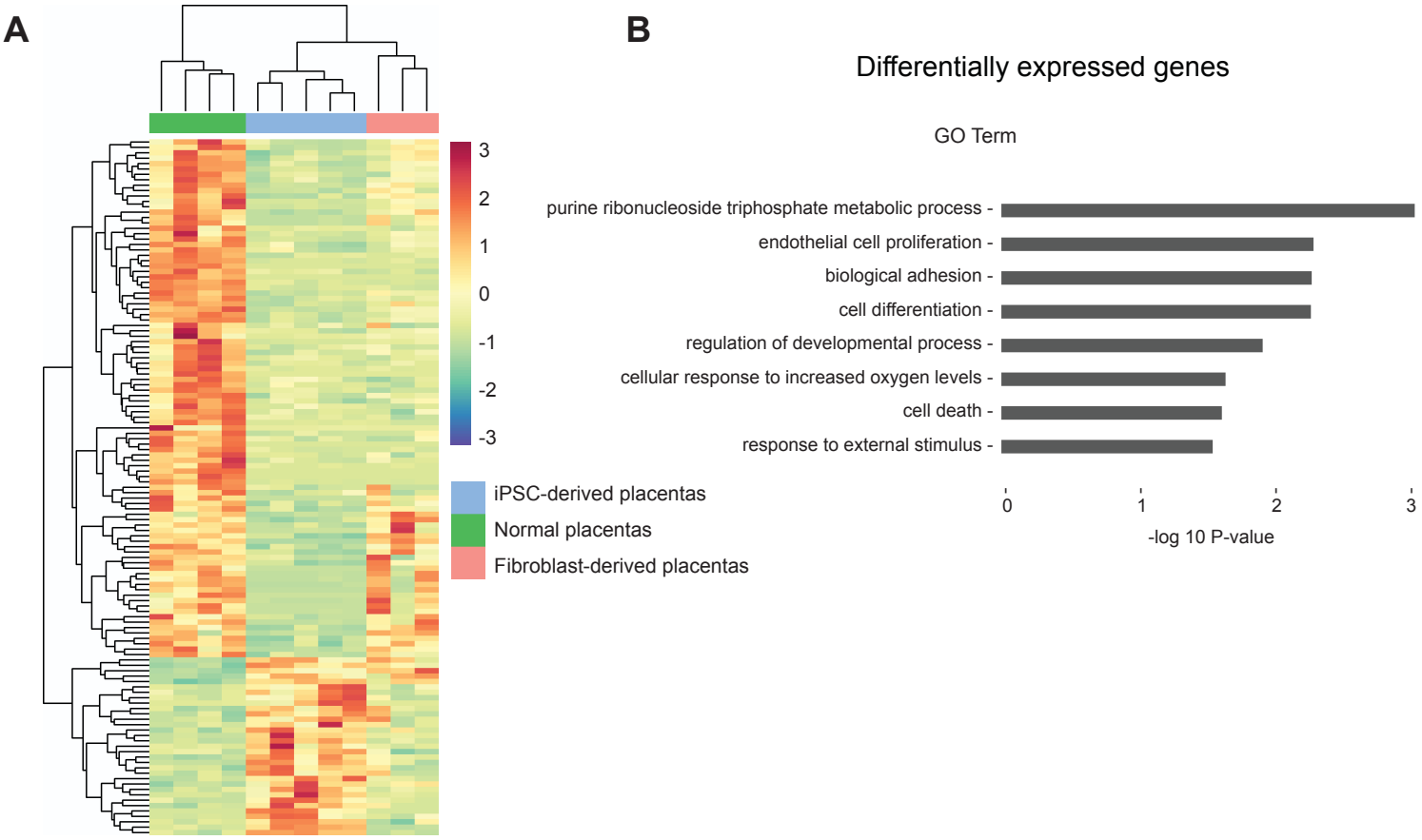
A
3
2
1
0
-1
-2
-3
iPSC-derived placentas
Normal placentas
Fibroblast-derived placentas
B
Differentially expressed genes
GO Term
purine ribonucleoside triphosphate metabolic process -
endothelial cell proliferation -
biological adhesion -
cell differentiation -
regulation of developmental process -
cellular response to increased oxygen levels -
cell death -
response to external stimulus -
0
1
2
3
-log 10 P-value

Fig. S8. Analysis of (DEGs) between iPSC-derived placentas and normal placentas.

(A) Heat map represents the expression profiles of DEGs between iPSC-derived placenta and normal placenta (DESeq2 adjusted P value, 0.001). Genes were subjected to hierarchical clustering.

(B) Gene ontology analysis of the DEGs between iPSC-derived placenta and normal placenta. The x-axis represents the negative log of the P values (classic Fisher's test) of the enrichment of the corresponding gene ontology terms.

Figure S9

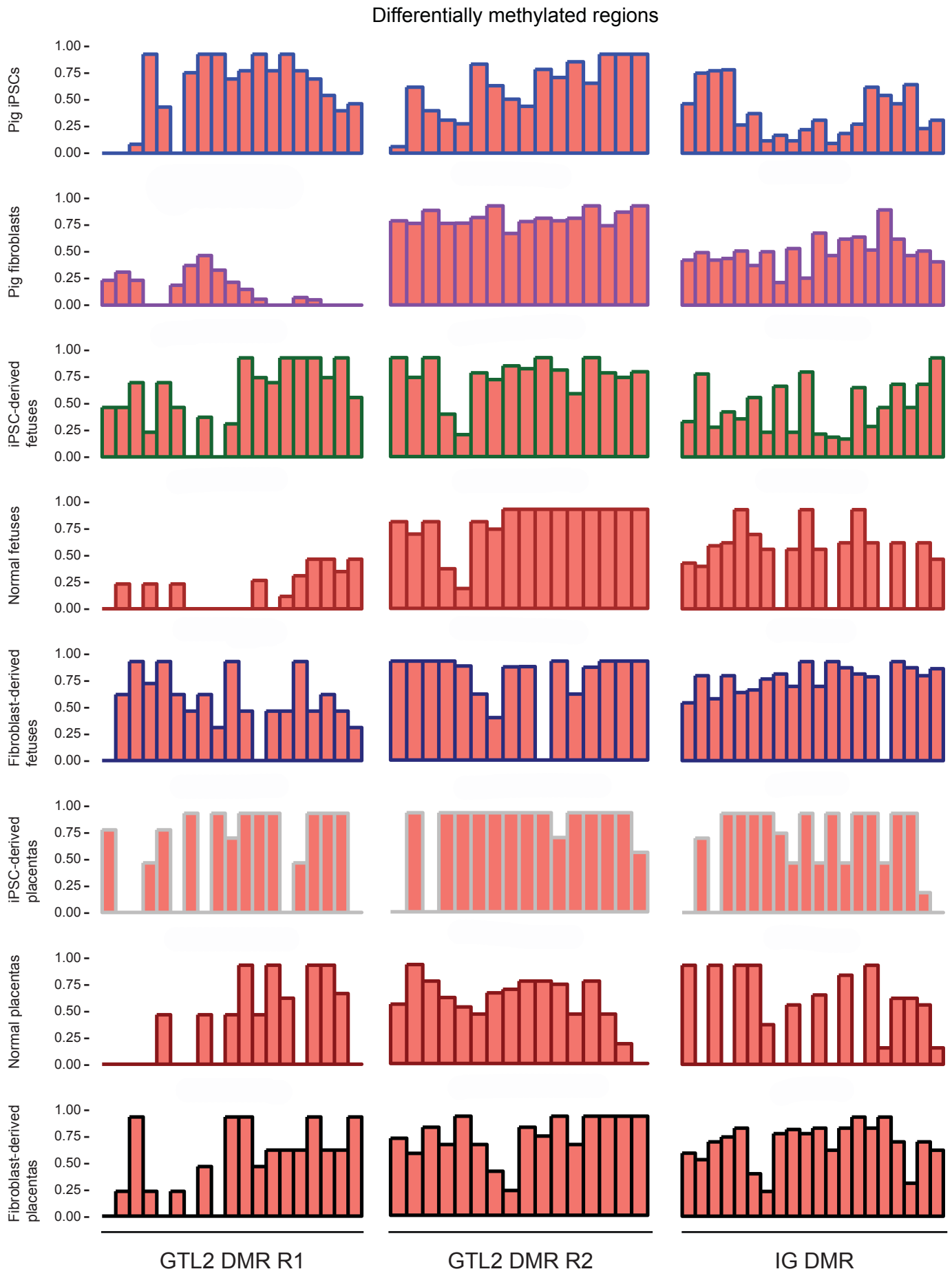
Differentially methylated regions
Pig iPSCs
Pig fibroblasts
iPSC-derived fetuses
Normal fetuses
Fibroblast-derived fetuses
iPSC-derived placentas
Normal placentas
Fibroblast-derived placentas
1.00
0.75
0.50
0.25
0.00
GTL2 DMR R1
GTL2 DMR R2
IG DMR

Fig. S9. Distribution of methylation levels across the *IG-GTL2* DMR region in the pig genome.

Each bar represents one CpG position, and the height shows the level of DNA methylation. The *GTL2* DMR R1 corresponds to the region Chr7: 132165384-132165582 in the pig genome. The *GTL2* DMR R2 corresponds to the region Chr7:132172903-132172954 in the pig genome. The *IG* DMR corresponds to the region Chr7: 132183855-132184138 in the pig genome. The iPSC-derived fetuses (placentas) show different levels of hypermethylation in the *GTL2* DMR and *IG* DMR.

Figure S10

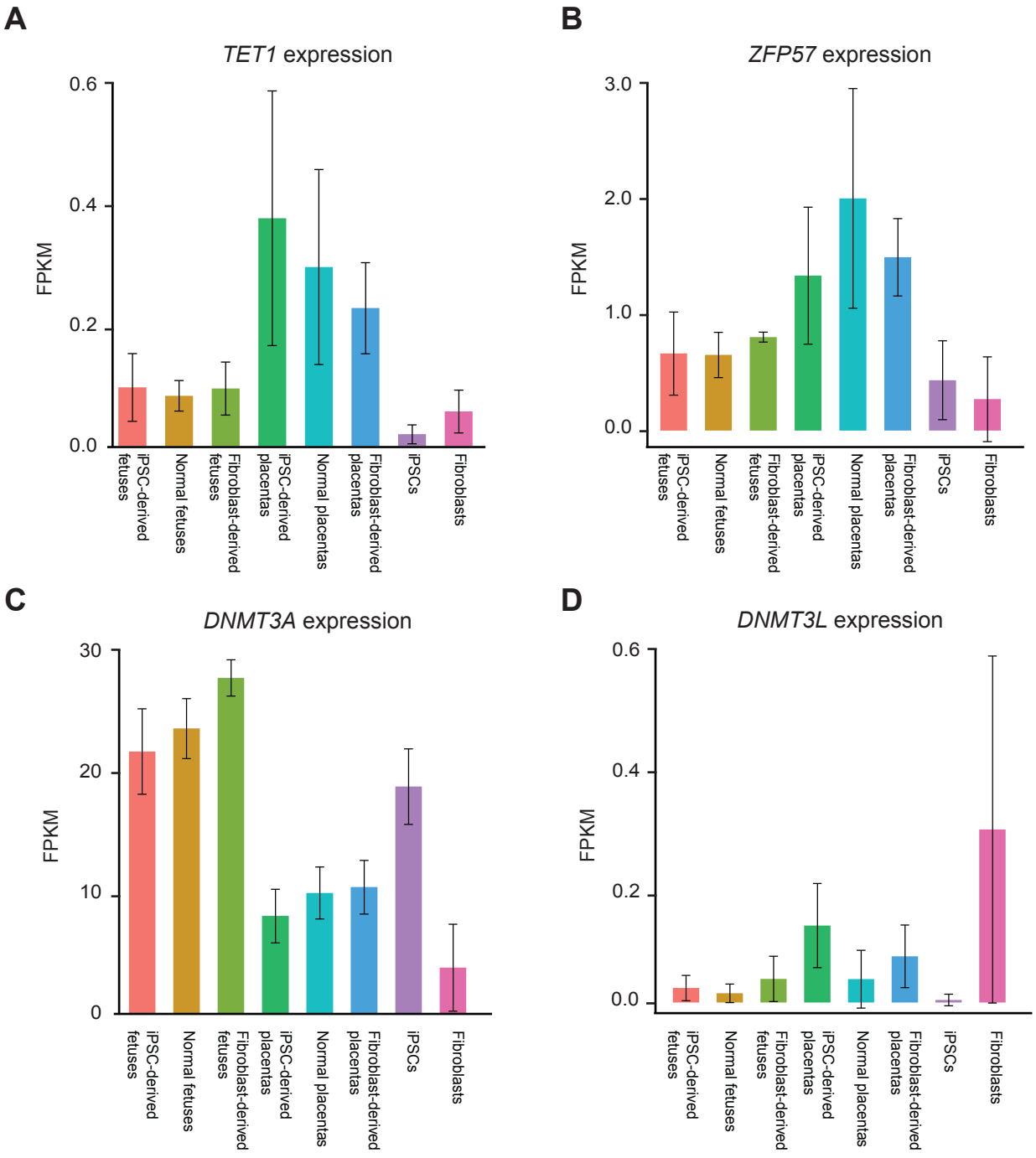
A
TET1 expression
FPKM
0.6
0.4
0.2
0.0
iPSC-derived fetuses
Normal fetuses
Fibroblast-derived fetuses
iPSC-derived placentas
Normal placentas
Fibroblast-derived placentas
iPSCs
Fibroblasts
B
ZFP57 expression
FPKM
3.0
2.0
1.0
0.0
iPSC-derived fetuses
Normal fetuses
Fibroblast-derived fetuses
iPSC-derived placentas
Normal placentas
Fibroblast-derived placentas
iPSCs
Fibroblasts
C
DNMT3A expression
FPKM
30
20
10
0
iPSC-derived fetuses
Normal fetuses
Fibroblast-derived fetuses
iPSC-derived placentas
Normal placentas
Fibroblast-derived placentas
iPSCs
Fibroblasts
D
DNMT3L expression
FPKM
0.6
0.4
0.2
0.0
iPSC-derived fetuses
Normal fetuses
Fibroblast-derived fetuses
iPSC-derived placentas
Normal placentas
Fibroblast-derived placentas
iPSCs
Fibroblasts

Fig. S10. Analysis of possible upstream genes of *RTL1* in different tissues.

(A) *TET1* expression in different tissues. No significant difference was detected between the iPSC-derived fetuses (placentas) and Normal fetuses (placentas).

(B) *ZNF57* expression in different tissues. No significant difference was detected between the iPSC-derived fetuses (placentas) and Normal fetuses (placentas).

(C) *DNMT3A* expression in different tissues. No significant difference was detected between the iPSC-derived fetuses (placentas) and Normal fetuses (placentas).

(D) *DNMT3L* expression in different tissues. No significant difference was detected between the iPSC-derived fetuses (placentas) and Normal fetuses (placentas).

Figure S11

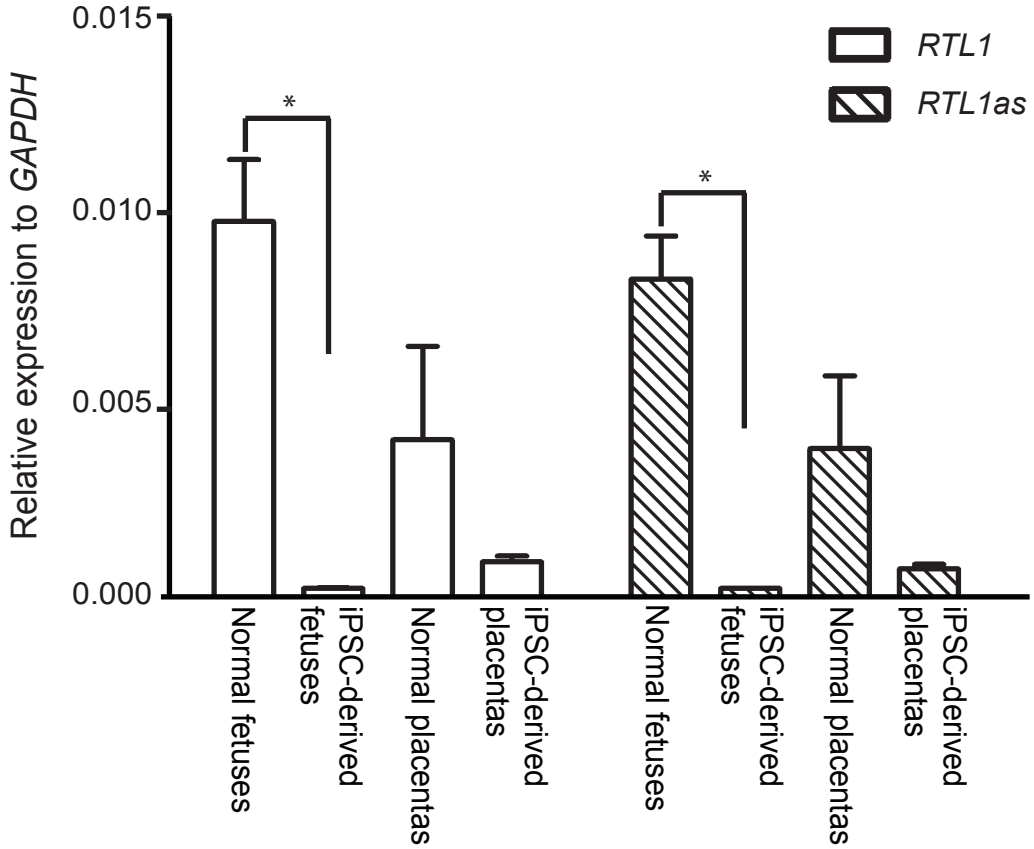
0.015
0.010
0.005
0.000
Relative expression to GAPDH
RTL1
RTL1as
*
*
Normal fetuses
iPSC-derived fetuses
Normal placentas
iPSC-derived placentas
Normal fetuses
iPSC-derived fetuses
Normal placentas
iPSC-derived placentas

Fig. S11 The expression of *RTL1* and *RTL1as* in Normal embryos and iPSC-derived embryos.

Similar amounts of *RTL1* and *RTL1as* transcripts were detected in normal embryos and iPSC-derived embryos. The data were representative of three independent experiments (mean ± SD). Statistical significance was analyzed by Student's t-test. *, $P < 0.05$; **, $P < 0.01$; ***, $P < 0.001$.

Figure S12

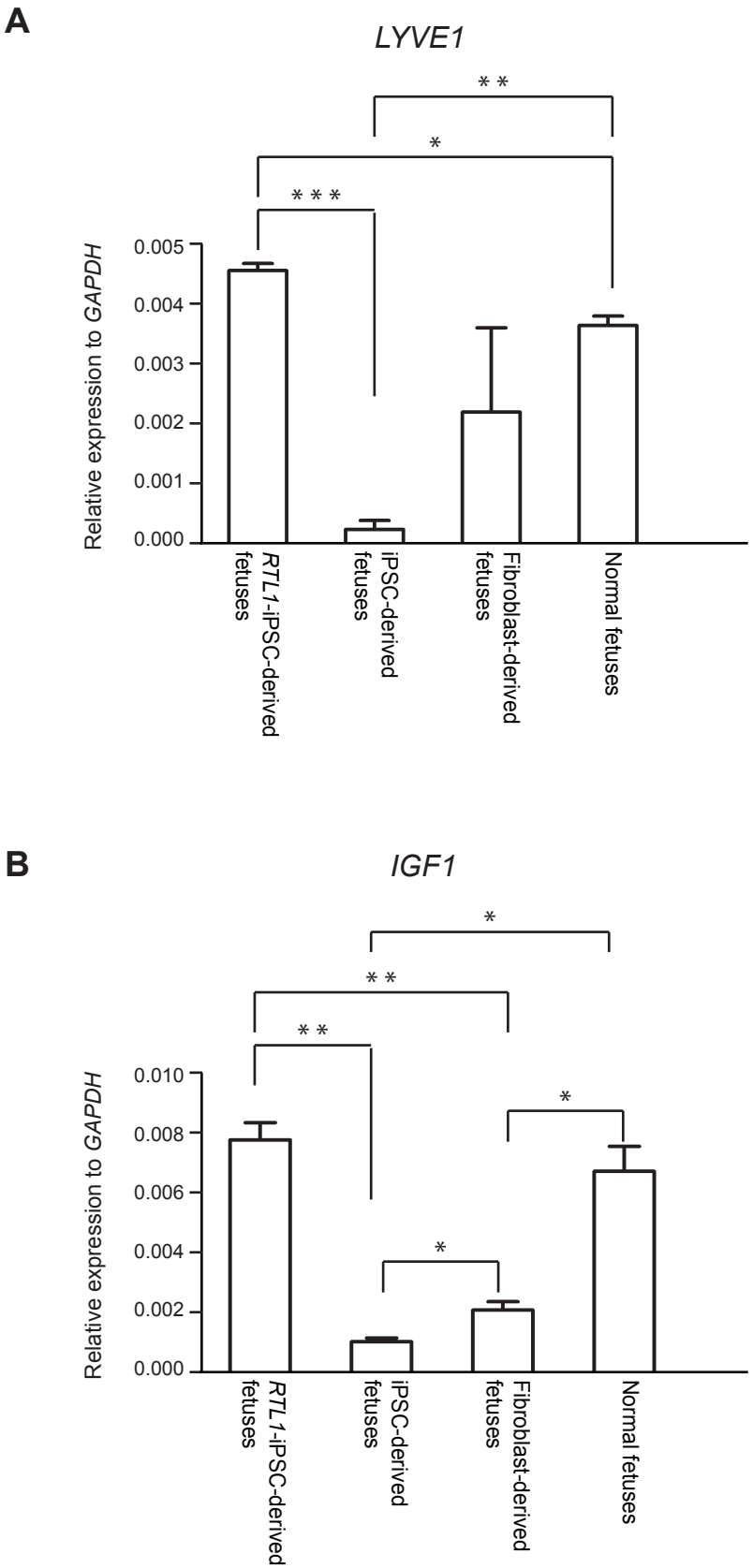
A
LYVE1
Relative expression to GAPDH
0.005
0.004
0.003
0.002
0.001
0.000
* *
*
* * *
RTL1-iPSC-derived fetuses
iPSC-derived fetuses
Fibroblast-derived fetuses
Normal fetuses
B
IGF1
Relative expression to GAPDH
0.010
0.008
0.006
0.004
0.002
0.000
*
* *
* *
*
*
RTL1-iPSC-derived fetuses
iPSC-derived fetuses
Fibroblast-derived fetuses
Normal fetuses

Fig. S12. Analysis of downstream genes of *RTL1* in different tissues.

(A) *LYVE1* expression in *RTL1*-iPSC-derived fetuses, iPSC-derived fetuses, fibroblast-derived fetuses and normal fetuses. The data were representative of three independent experiments (mean ± SD). Statistical significance was analyzed by two-tail Student's t-test. *, $P < 0.05$; **, $P < 0.01$; ***, $P < 0.001$.

(B) *IGF1* expression in *RTL1*-iPSC-derived fetuses, iPSC-derived fetuses, fibroblast-derived fetuses and normal fetuses. The data were representative of three independent experiments (mean ± SD). Statistical significance was analyzed by two-tail Student's t-test. *, $P < 0.05$; **, $P < 0.01$; ***, $P < 0.001$.

Figure S13

A

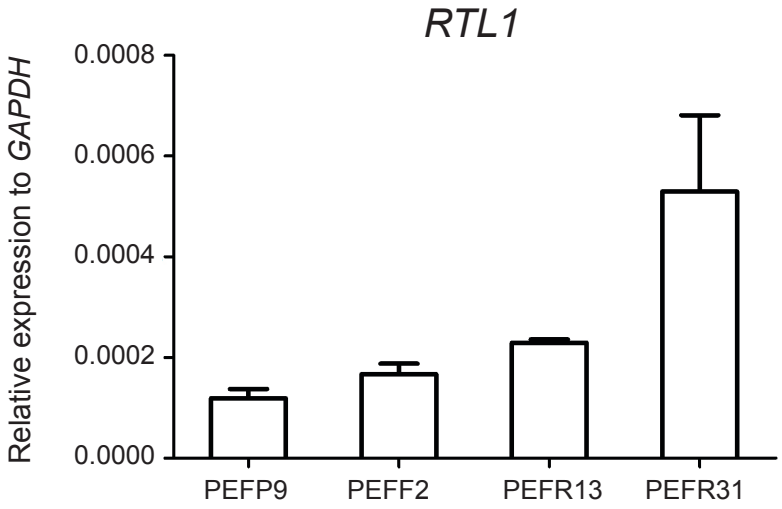

B

In vivo development of nuclear transfer embryos derived from fibroblasts

Donor cells	NO. of transferred embryos	NO. of recipients	NO. of pregnancies
PEFP9	1230	5	0
PEFF2	1250	4	0
PEFR13	775	3	2
PEFR31	2895	8	5

Fig. S13. A positive correlation between the expression of *RTL1* and cloning efficiency in pig fibroblast.

(A) The expression of *RTL1* in four fibroblast cell lines that have been showed different cloning efficiency. The data were representative of three independent experiments (mean ± SD).

(B) *In vivo* development of nuclear transfer embryos derived from four fibroblast cell lines.

A positive correlation was shown between the expression of *RTL1* and cloning efficiency (Spearman Rank Correlation, 0.58).

Figure S14

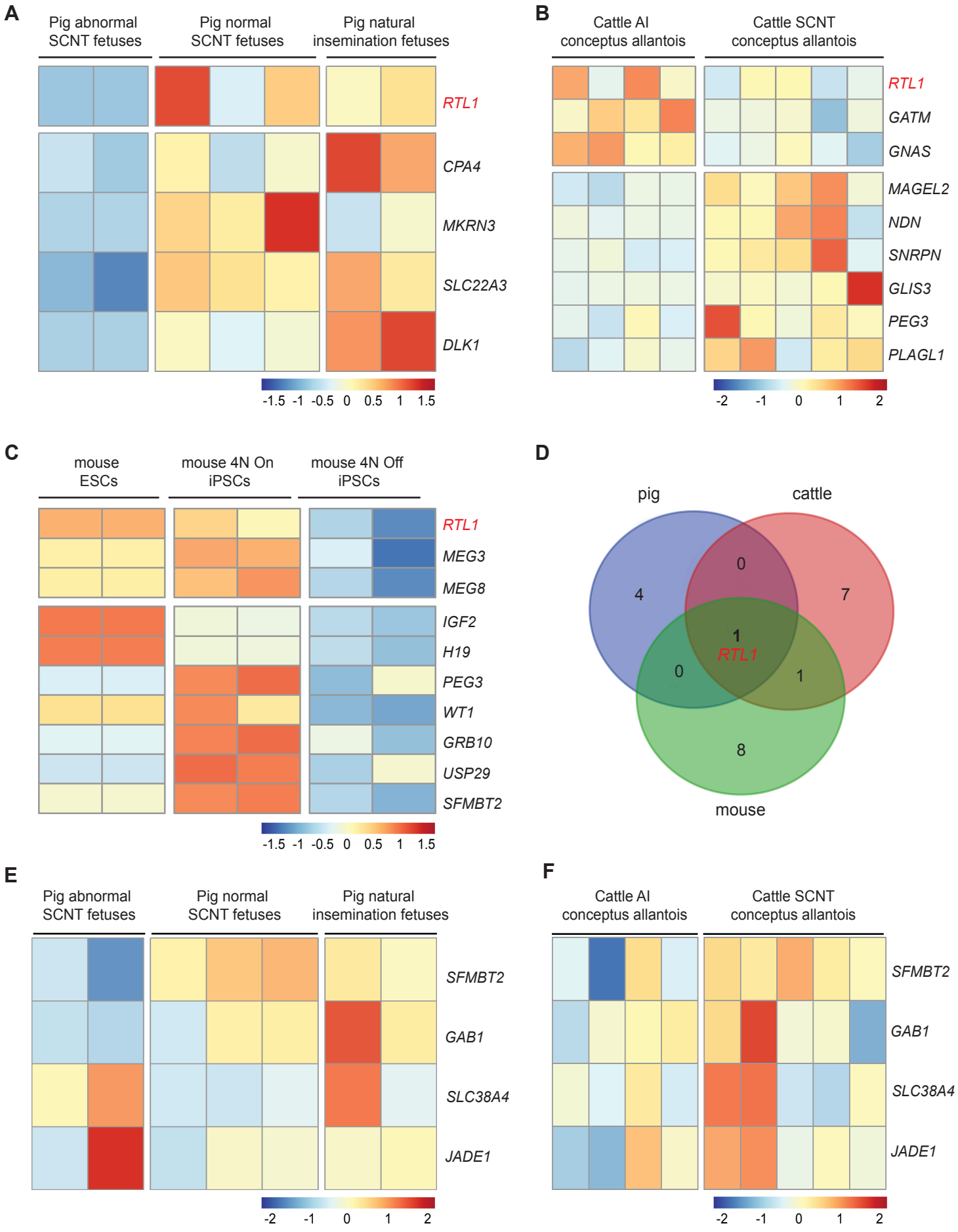
A
Pig abnormal SCNT fetuses
Pig normal SCNT fetuses
Pig natural insemination fetuses
RTL1
CPA4
MKRN3
SLC22A3
DLK1
-1.5 -1 -0.5 0 0.5 1 1.5
B
Cattle AI conceptus allantois
Cattle SCNT conceptus allantois
RTL1
GATM
GNAS
MAGEL2
NDN
SNRPN
GLIS3
PEG3
PLAGL1
-2 -1 0 1 2
C
mouse ESCs
mouse 4N On iPSCs
mouse 4N Off iPSCs
RTL1
MEG3
MEG8
IGF2
H19
PEG3
WT1
GRB10
USP29
SFMBT2
-1.5 -1 -0.5 0 0.5 1 1.5
D
pig
cattle
mouse
4
0
7
1
RTL1
0
1
8
E
Pig abnormal SCNT fetuses
Pig normal SCNT fetuses
Pig natural insemination fetuses
SFMBT2
GAB1
SLC38A4
JADE1
-2 -1 0 1 2
F
Cattle AI conceptus allantois
Cattle SCNT conceptus allantois
SFMBT2
GAB1
SLC38A4
JADE1
-2 -1 0 1 2

Fig. S14. *RTL1* is the most frequent abnormally expressed gene among all aberrant imprinted genes across different species.

(A) Heat map represents the expression profiles of differentially expressed imprinted genes between the abnormal SCNT fetuses and normal fetuses in pigs. The heatmap is scaled by row. ($P < 0.05$, two-tailed Student's t-test).

(B) Heat map represents the expression profiles of differentially expressed imprinted genes between SCNT conceptuses and four artificial insemination (AI) conceptuses in cattle (DESeq2 P value, 0.05). The imprinted gene in cattle was inferred from the homologous imprinted gene in the mouse.

(C) Heat map represents the expression profiles of differentially expressed imprinted genes between 4N-competent iPSC and 4N-incompetent iPSC in mouse (DESeq2 adjusted P value, 0.1, log2 fold change > 1).

(D) A Venn diagram shows the number of differentially expressed imprinted genes in panels A-C.

(E) Heat map represents the expression profiles of four H3K27me3 dependent imprinted genes between the abnormal SCNT fetuses and normal SCNT fetuses in pigs. The heat map is scaled by row (two-tailed Student's t-test was performed on these genes between abnormal pig SCNT fetuses and normal SCNT fetuses. *SFMBT2*, P = 0.11; *GAB1*, P = 0.30; *SLC38A4*, P = 0.66; *JADE1*, P = 0.31).

(F) Heat map represents the expression profiles of four H3K27me3 dependent imprinted genes

between NT conceptuses and four artificial insemination (AI) conceptuses in cattle (Statistical tests were conducted with DESeq2 P value. *SFMBT2*, P = 0.093; *GAB1*, P = 0.68; *SLC38A4*, P = 0.36; *JADE1*, P = 0.31). The four H3K27me3 dependent imprinted genes were inferred from the homologous imprinted genes in the mouse.

Figure S15

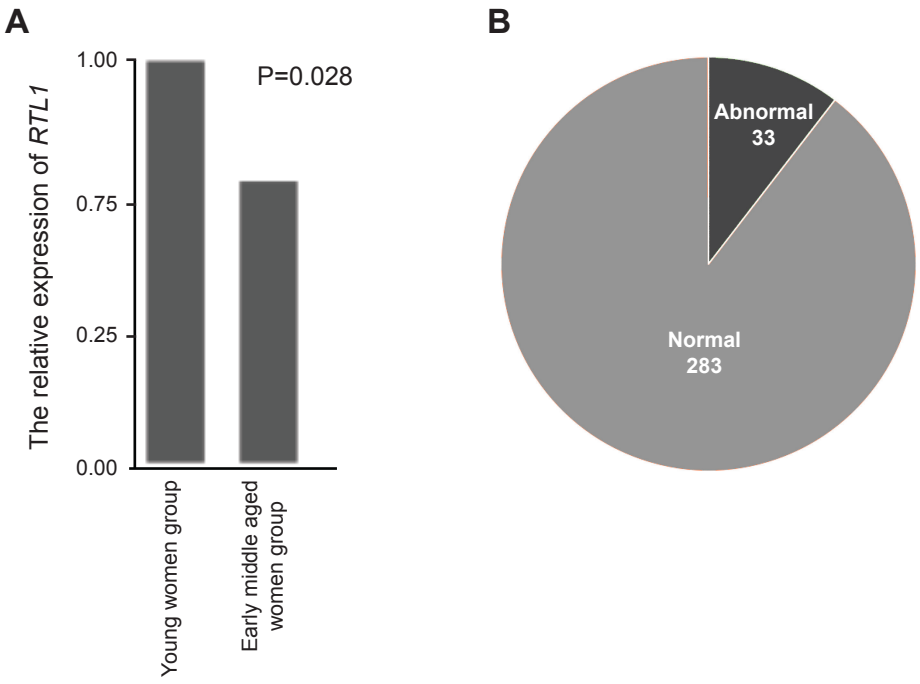
A
1.00
0.75
0.25
0.00
P=0.028
The relative expression of RTL1
Young women group
Early middle aged women group
B
Abnormal
33
Normal
283

Fig. S15. Analysis of data in previous studies shows a correlation of low RTL1 expression and human fertility problems.

(A) The relative expression of *RTL1* in human 1st trimester placental chorionic villi with different maternal age. The young women group includes placentas from women of 18, 19, 21 and 24 years, and the early middle-aged women group includes placentas from women of 27, 30, 32 and 33 years. The expression of *RTL1* was scaled according to gene expression in the young women group.

(B) The occurrence of abnormal methylation at *GTL2* DMR in the sperm from male patients with fertility problems.

Figure S16

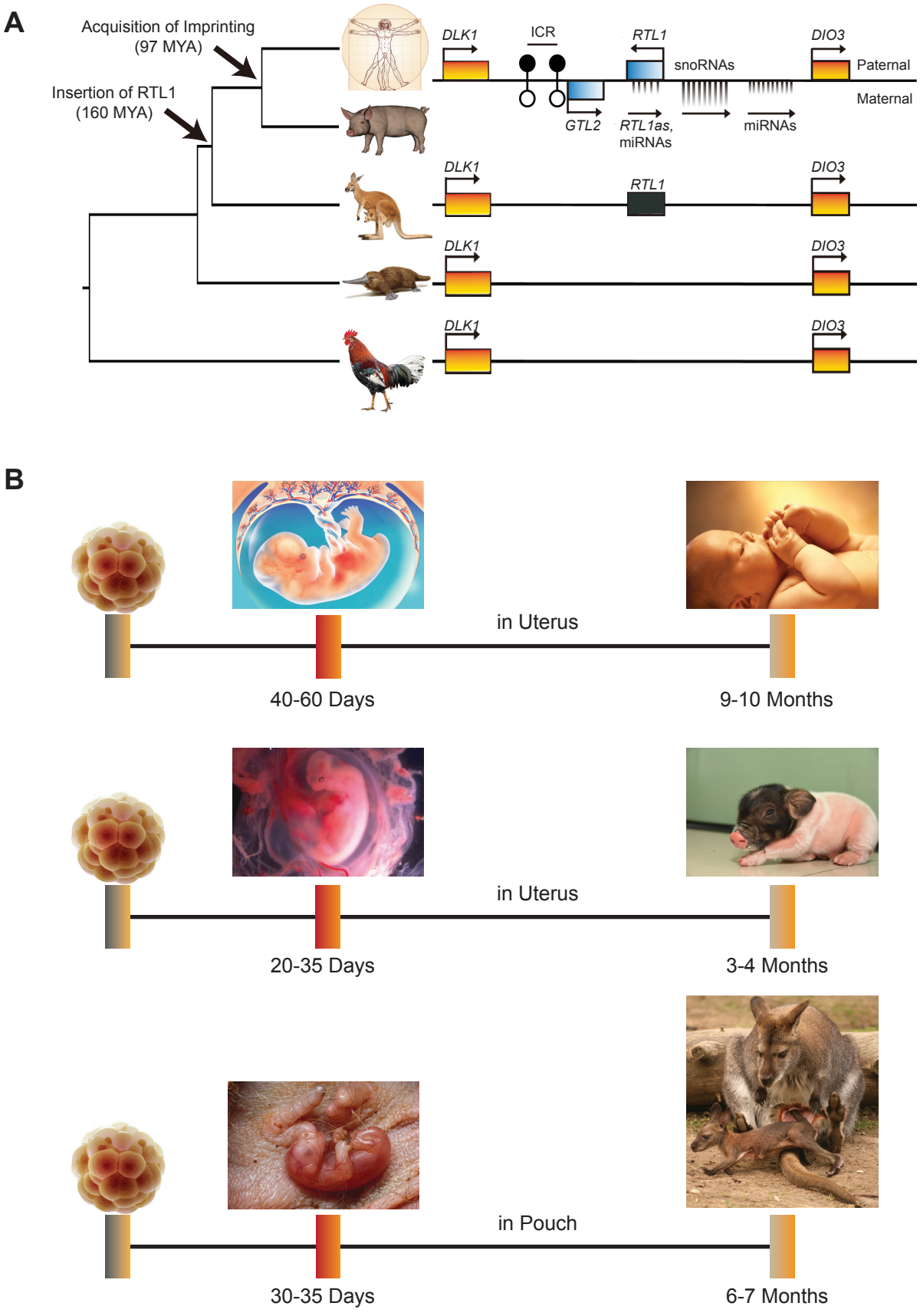
A
Acquisition of Imprinting
(97 MYA)
Insertion of RTL1
(160 MYA)
DLK1
ICR
RTL1
DIO3
snoRNAs
Paternal
Maternal
GTL2
RTL1as,
miRNAs
miRNAs
B
in Uterus
40-60 Days
9-10 Months
in Uterus
20-35 Days
3-4 Months
in Pouch
30-35 Days
6-7 Months

Fig. S16. *RTL1* holds an important status in mammalian evolution.

(A) A phylogenetic tree of five vertebrates. The main evolutionary events are marked (MYA, million years ago). The right panel is a schematic representation of the *DLK1-DIO3* domain in human, pig, wallaby, platypus, and chicken showing evolutionary changes in the locus. *RTL1* was inserted into the domain in the common ancestor of wallaby, pig and human and then became imprinted and functional in Eutheria (human and pig), accompanied by the acquisition of imprinting control regions (ICR). The imprinting control region for the domain is the paternally methylated *IG*-DMR and *GTL2*-DMR. Filled circles, methylated; open circles, unmethylated.

(B) Schematic of full-term pregnancy in human, pig, and wallaby. Normally, if the eutherian embryo establishes a fetomaternal interface at the indicated stages, it can survive to term. Otherwise, the embryo is resorbed early. In the wallaby, embryos develop in the pouch and do not require formation of the fetal-maternal connection after 30-35 days in uterus development.

Table S1. Comparison of in vivo development of cloned and normal pig embryos

Embryo source	No. of transferred embryos	No. of recipients	No. of pregnancies				No. of live piglets
			GD25	GD45	GD60	full term	
Natural fertilized embryos	-	10	9 (91.6±14.4%)[a]	9 (91.6±14.4%)[a]	9 (91.6±14.4%)[a]	9 (91.6±14.4%)[a]	66
Fibroblasts-derived embryos	5307	20	15 (73.6±12.0%)[a]	14 (68.1±18.8%)[b]	14 (68.1±18.8%)[b]	14 (68.1±18.8%)[b]	69 (1.2±0.4%)[a]
iPSC-derived embryos	2959	16	5 (31.1±10.2%)[b]	1 (5.6±9.6%)[c]	1 (5.6±9.6%)[c]	0(0)[c]	0(0)[b]

[a,b,c] Values with different superscripts represent significant differences of pregnancy rate within the same column ($P < 0.05$).